EFFICIENT AND ACCURATE AEROELASTIC ANALYSES BASED ON SMALL-DISTURBANCE CFD IN EARLY AIRCRAFT DEVELOPMENT

Cyrille Vidy[1], Lukas Katzenmeier[1], Maximilian Winter[2], Christian Breitsamter[2]

[1] Airbus Defence and Space, Structural Dynamics (Aeroelasticity) TAEGD2
Rechliner Strasse, D-85077 Manching, Germany
cyrille.vidy@airbus.com
lukas.katzenmeier@tum.de

[2] Chair of Aerodynamics and Fluid Mechanics, Technical University of Munich
Boltzmannstr. 15, D-85748 Garching, Germany
Maximilian.Winter@aer.mw.tum.de
Christian.Breitsamter@aer.mw.tum.de

Keywords: Aeroelasticity, Structural Dynamics, Small-Disturbance CFD, AIC-correction, Dynamic Coupling

Abstract: This paper presents several methods which are useful to reduce the number of small-disturbance CFD computations needed for the production of more accurate datasets for aeroelastic analyses in early aircraft development.

The first method presented here is an AIC-correction technique using the results of a few small-disturbance CFD computations in order to generate downwash correction matrices for panel methods such as Doublet-Lattice or ZONA51 in MSC-NASTRAN [5].

The other two methods are based on a component-wise modal basis-technique similar to branch-mode techniques [3] and on the reuse of the modal basis of a given mass-state of an aircraft for dynamic and aeroelastic analyses at other mass states.

All these methods are proven to be efficient, accurate and robust, and the authors show the potential reduction of the computational effort for concrete analysis cases by means of a generic MALE-configuration: OptiMALE.

1 INTRODUCTION

In a cooperation between the Technical University of Munich and Airbus Defence and Space, the small-disturbance CFD tool AER-SDNS has been developed. It is based on the analytic linearization of the fluid dynamic equations (Euler or RANS) around a nonlinear steady reference state. It can generate first order harmonic aerodynamics out of modal deformations or of gust excitations. It generates generalized aerodynamic forces in the same form as classical aerodynamic tools as Doublet-Lattice Method (DLM) [4] or ZONA51 in MSC-NASTRAN [5], as well as non-generalized results if needed. Thus the results can be used with actual aeroelastic certification requirements and linear analysis tools for static and dynamic aeroelastic stability and loads [1].

Small-disturbance CFD has proven to be a very efficient way for computing linearized CFD aerodynamics for aeroelastic analyses. However, despite its high efficiency compared to other

CFD solutions, the generation of a complete AER-SDNS dataset can take from a few days to some weeks. An AER-SDNS computations can namely last several hours and the number of AER-SDNS computations required for the creation of a complete dataset equals namely the product of the number of Mach numbers, reduced frequencies and eigenmodes of interest for each flight condition considered (angle of attack, control surfaces positions). Especially during the development process of new airplanes, the main limitation of this approach is the computational effort needed to obtain the full AER-SDNS dataset in order to analyze the considered configuration(s). The present work intends to overcome this serious limitation and to smooth the ramp-up of the introduction of the CFD-dataset during early development phases of an aircraft.

2 PROPOSED SMALL-DISTURBANCE CFD ACCELERATION METHODS

2.1 AIC-correction

In the past, several authors developed correction techniques (e.g. [2]) using mostly steady CFD or experimental data for a correction with multiplicative or additive correction matrices. Until now, most of the authors employ either diagonal or densely populated matrices. The authors developed a correction method based on a multiplicative approach for a DLM downwash correction using densely populated correction matrices with dominant diagonal entries. This approach enables the introduction of data from multiple modes at a time, increases the accuracy compared to other correction techniques, and it minimizes the qualitative change posed to the distribution of aerodynamic quantities.

The correction technique is based on an identity of the corrected DLM forces and the small-disturbance forces obtained with AER-SDNS normal to the DLM panels. Only the pressure disturbance part of the forces from AER-SDNS is considered here, since classical Doublet-Lattice Methods do not consider other force components resulting from the steady pressure difference and the surface vector disturbance. An additive correction can be applied to account for such components, but is beyond the scope of the present paper. Due to the nature of the results of the aerodynamic methods, the correction matrix is complex and depends on reduced frequency, Mach number and flight condition. The identity of forces reads:

$$\boldsymbol{G}^T\boldsymbol{F}_{SD} = \boldsymbol{S}\cdot\boldsymbol{AIC}\cdot\boldsymbol{C}_W\frac{\boldsymbol{W}}{U_\infty} \tag{1}$$

In equation 1, $\mathbf{C_w}$ is the correction matrix correcting the downwash of the DLM. $\mathbf{G^TF_{SD}}$ are the normal parts of the AER-SDNS forces transformed to the DLM lifting points using Infinite Plate Splines. **S** is the diagonal matrix of the panel surfaces and **W** is the downwash vector. $\mathbf{C_w}$ consists of a diagonal part $\boldsymbol{\Lambda}$ and off-diagonal entries $\boldsymbol{\Delta}$:

$$\boldsymbol{C}_W = \boldsymbol{\Lambda}\left(k_{red},\, Ma_\infty\right) + \boldsymbol{\Delta}\left(k_{red},\, Ma_\infty\right) \tag{2}$$

For shorter notation, it is $\boldsymbol{W}_a = \boldsymbol{AIC}^{-1}\boldsymbol{S}^{-1}\boldsymbol{G}^T\boldsymbol{F}_{SD}$ and $\boldsymbol{W}_b = \boldsymbol{W}/U_\infty$ in the following. First, the diagonal part is computed by solving the over-determined system

$$\boldsymbol{W}_a = \begin{bmatrix}\lambda_1 & & 0\\ & \ddots & \\ 0 & & \lambda_n\end{bmatrix}\boldsymbol{W}_b \tag{3}$$

with a least-squares approach (Gaussian Transformation). The remaining difference between the diagonal correction results and the small-disturbance forces from AER-SDNS is covered by the off-diagonal entries through a Moore-Penrose pseudo-inverse:

$$\boldsymbol{\Delta} = (\boldsymbol{W}_a - \boldsymbol{\Lambda} \cdot \boldsymbol{W}_b) \cdot [(\boldsymbol{W}_b^H \cdot \boldsymbol{W}_b)^{-1}]^H \boldsymbol{W}_b^H \quad (4)$$

The obtained matrix C_w can then be built using several "training eigenmodes", or columns of $\mathbf{W_a}$ and $\mathbf{W_b}$, simultaneously. Typically, one can use the flight mechanical eigenmodes of the configuration, elastic eigenmodes and also some control surfaces deformations in order to obtain an appropriate correction matrix. It can be also defined for nonzero reduced frequencies, avoiding the need of any assumption on the behavior of the correction along the reduced frequencies.

Since some training eigenmodes can lead to values close to zero at low frequencies (e.g. plunge mode), one can take advantage of the computation of the Moore-Penrose pseudo-inverse with the help of the Singular Value Decomposition. Using a tolerance value for the minimum considered singular value can ensure that a dataset (column in W_a and W_b) is ignored when it shows values close to 0 in comparison to other training modes. This regularization of the pseudo-inverse makes the creation of the correction matrix very robust and user-friendly.

Also, an interesting feature for half models is the intended symmetry of the correction: a box of the aerodynamic model on one side of a symmetric configuration should be corrected exactly as its symmetric counterpart. One can derive from this symmetry that one should use the same correction matrix for symmetric and antisymmetric results. Then this correction matrix can be trained using simultaneously with symmetric and antisymmetric data, e.g. with all 6 rigid-body modes, even if only antisymmetric computations are intended.

One should still keep in mind that this method is a correction technique and thus not intended to recreate effects missed by DLM as transonic shocks or some T-tail aerodynamics. For the latter, the following modal basis improvement methods can be considered.

2.2 Component-wise modal basis

For the early development phase of an aircraft, the chosen modal basis should allow to consider a full CFD-dataset for a limited amount of specific eigenmodes. The remaining eigenmodes should be covered with classical generalized aerodynamics coming from DLM or ZONA51. An AIC-correction technique should be applied to these results in order to smooth the discrepancies with CFD.

The current approach is inspired by the Branch-Modes Modelling technique [3]. One can build a modal basis using the dynamic coupling between a master part and one or several slave parts that can be used in order to isolate the elastic effects of some structural part.

For OptiMALE, the T-tail has been isolated and its eigenmodes were computed when it was clamped at its fixation points. The rest of the model was computed with a rigid T-tail in order to consider the effect of its mass on the fuselage eigenmodes. This rigid T-tail was realized using a RBE2-element of NASTRAN between the node (master node) representing the mass properties of the full T-tail and the fixation points (slave nodes).

In a second step, the modal basis issued of the eigenmodes of these both computations was created and the eigenmodes of the full configuration are compared with the ones rebuilt using the component-wise modal basis.

2.3 Reuse of modal bases

In the later development phase, the main differences between configurations arise from varying payloads, fuel states and some local mechanical effects. This results in limited variations in modal results and also in many similarities with respect to the aeroelastic results.

The use of the modal basis of one or of a few representative configurations (e.g. a maximum take-off weight configuration) for the generation of the generalized aerodynamic forces of the remaining configurations can be very efficient whereas the prediction error is limited.

This method has been already used by Airbus Defence and Space in the past and is demonstrated in this paper, while three different fuel states are considered as the reference configuration for each other.

3 COMPUTATIONAL MODEL: THE OPTIMALE CONFIGURATION

The OptiMALE configuration has been chosen by the authors in order to demonstrate the methods presented in this paper. It has already been used by the authors in the past in order to demonstrate the integration of small-disturbance CFD into the aeroelastic analysis [1]. Thus, only a short summary of its characteristics is presented here.

The OptiMALE configuration by Airbus Defence and Space represents a generic MALE with high aspect-ratio wing, T-tail empennage, fuselage mounted engines and wing-mounted external fuel tanks. Additionally, internal fuel tanks are located in the fuselage and in the wing.

The structured CFD-mesh (Figure 1) represents the right half of the configuration and consists of approximately 7 million hexa-mesh cells. In accordance with the aerodynamic modelling using the Euler-equations, an offbody-distance of $OBD = 10^{-3} \cdot l_r$ was used.

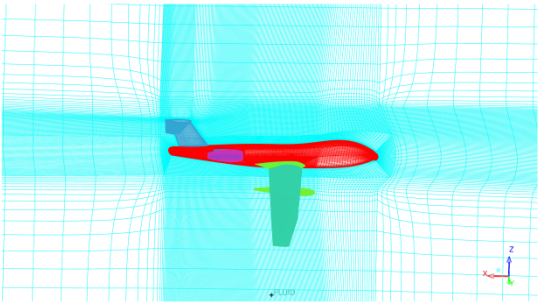

Figure 1: Side-view of the AER-SDNS OptiMALE CFD-mesh.

The FEM-model (Figure 2) used for the analysis is very detailed. It also represents the right half of the configuration, whereas the engine and external store are simply represented as

mass points. It can be used for symmetric and antisymmetric analyses by applying the appropriate set of Single Point Constraints at the symmetry plane of the configuration, producing the adequate modal bases for aeroelastic analyses.

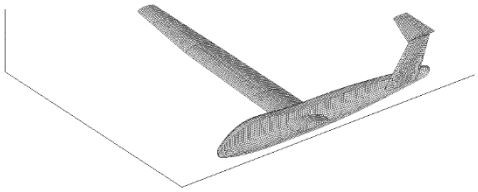

Figure 2: OptiMALE FEM-model.

The coupling between both meshes is given in reference [1]. It uses Thin-Plate-Splines for the model surface deformation, and a combination of spring analogy and transfinite interpolation for the volume deformation of the CFD-mesh.

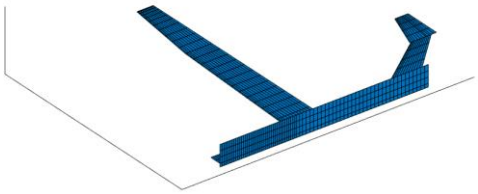

Figure 3: OptiMALE DLM-model.

The Doublet-Lattice model (Figure 3) used for this paper is also a half-model. It consists of approximatively 850 boxes and includes a horizontal and a vertical paneling of the fuselage. The external fuel tank, the engine and their stores have been neglected here. The fluid-structure coupling for the DLM model has been realized with Infinite-Plate-Splines.

4 RESULTS

In the following, antisymmetric modal and flutter results of the OptiMALE configuration are presented. The AIC-correction and the component-wise modal basis techniques are presented for the Maximum Take-Off Weight case (MTOW) at Mach 0.4.

4.1 AIC-correction

The modal basis used for the generation of generalized aerodynamic forces is the component-wise modal basis that will be discussed in more details in section 4.2. The training of the AIC-correction for OptiMALE used all 6 (symmetric and antisymmetric) rigid-body modes of the OptiMALE half-model at Mach 0.4 for 9 reduced frequencies between k_{red}=0.01 and k_{red}=5. This ensures that every box of the Doublet-Lattice model gets a non-zero downwash for at least some modes in the whole reduced frequency range, making the training of the AIC-correction very robust.

4.1.1 Correction matrices

The CFD surface nodes have been grouped in order to associate them to the Doublet-Lattice panels as shown in figure 4 for the AIC-correction. Thus, the resulting CFD forces will be fully used for the corresponding Doublet-Lattice panels and not for other parts of the model, as would be the case if one overall spline had been defined here. The forces at the external fuel tank and at the engine (and their respective pylons) are ignored since they have no counterpart in the current DLM-mesh.

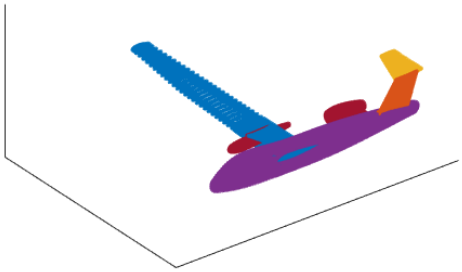

Figure 4: Zones of the AER-SDNS mesh for the AIC-correction

The computed correction matrices are, as expected, strongly diagonal for all reduced frequencies, so that the authors decided to present more precisely the diagonal of the correction matrix for two reduced frequencies (k_{red}=0.01 and k_{red}=0.5) in Figure 5. The real part is plotted with a full line, whereas the imaginary part is plotted with a dashed line.

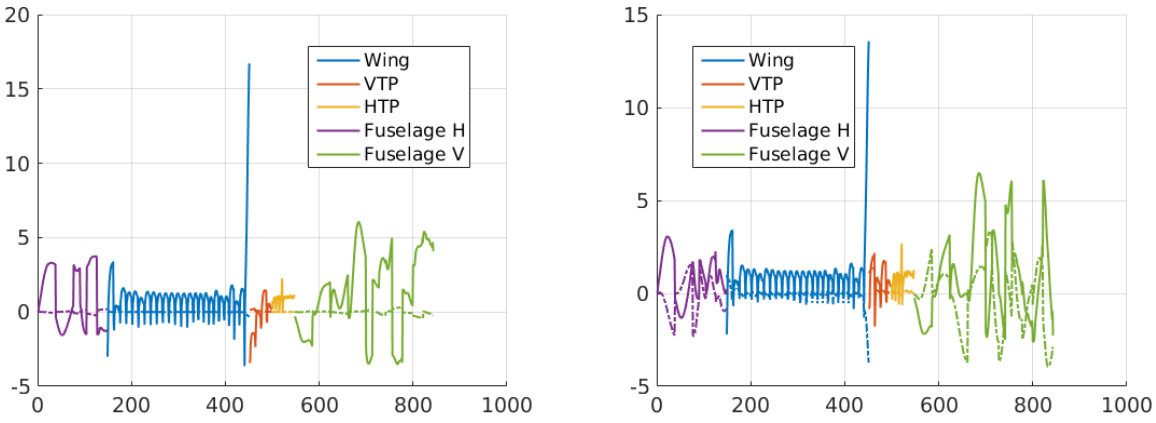

Figure 5: Diagonal of the downwash correction matrix for k_{red}=0.01 (left) and k_{red}=0.5 (right)

One can see that the AIC-correction for the lifting surfaces (wing, horizontal tail plane and vertical tail plane) shows the expected behavior that was already observed in past studies [2]. The real part lies slightly above 1.0 and decreases at the leading and trailing edges boxes. The imaginary part is close to 0, showing that the frequency dependency of the aerodynamics is similar for DLM and AER-SDNS (Euler). The high peak corresponds to the DLM-box at the wing tip trailing edge, which has a negligible aerodynamic effect on the rest of the wing.

For the fuselage boxes, the correction is quite different, which is understandable given that the paneling of an aerodynamic body is a less accurate modelling of it.

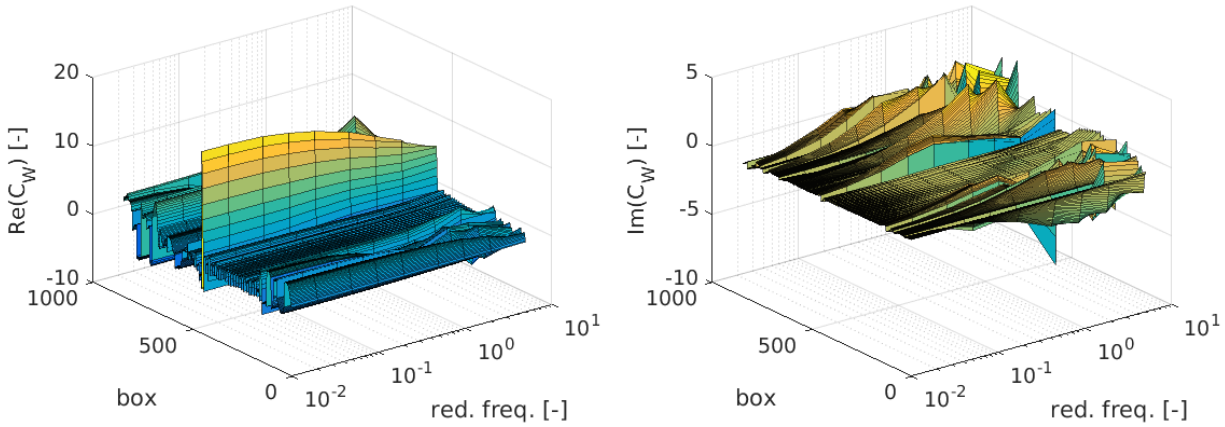

Figure 6: Variation of the diagonal of the correction matrix along the reduced frequency

The variation of the diagonal coefficients of the downwash correction matrix with the reduced frequency can be found in Figure 6. It can be observed that this variation is smooth, thus it could be even possible to compute the AIC-correction for some reduced frequencies and to interpolate it at other values. This would further reduce the number of small-disturbance CFD analyses needed for the training of the AIC-correction.

4.1.2 Generalized aerodynamics

In order to evaluate the effects of the AIC-correction, one can compare the generalized forces obtained with AER-SDNS (dashed lines), DLM (dotted lines) and DLM with AIC-correction (full lines, see Figure 7).

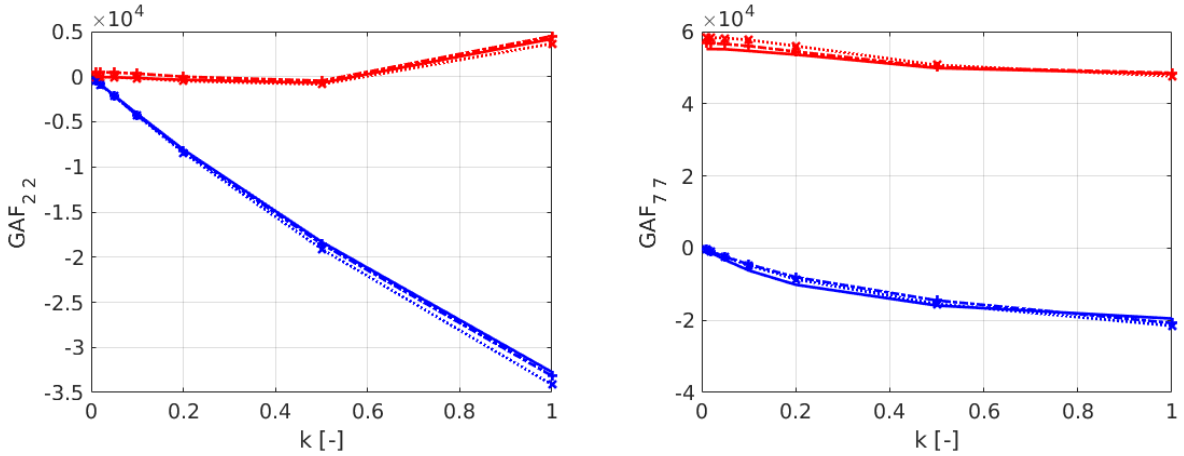

Figure 7: GAF versus reduced frequency: AER-SDNS (+), DLM (x) and DLM corrected (full lines)

On the left side of Figure 7, one can see the effect of the AIC-correction on the GAF element of a training mode. The corrected GAF value is closer to the AER-SDNS GAF in this case. The discrepancies can be explained with the following points:

- Only the normal components of the AER-SDNS pressure disturbance force are used for the AIC-correction
- The disturbance force due to the surface vector disturbance considered in AER-SDNS is ignored here. It could be added (at least for the forces normal to the box) in terms of an additive GAF-correction.

On the right side of Figure 7, one can see the effect of the AIC-correction on a non-training mode. The GAF element of the corrected DLM does not match perfectly the AER-SDNS results, which can be explained by the arguments already given. An overall positive effect compared to the GAFs from the DLM can still be observed. A more general observation of the GAF entries of all modes was that the AIC-correction did mostly reduce the difference with AER-SDNS GAFs, and had no remarkable negative effect on any of the GAF-coefficients.

4.1.3 Flutter results

The flutter analysis of the OptiMALE configuration has been done for Mach 0.4 at Sea Level. In this section, the results using three different GAF-datasets are compared:

- Full small-disturbance CFD GAFs (all 22 antisymmetric modes)
- AIC-corrected Doublet-Lattice GAFs (trained with the 6 rigid-body modes)
- Non-corrected Doublet-Lattice GAFs

Figure 8 shows the results of the first two cases, the last one can be seen in Figure 13 (right side).

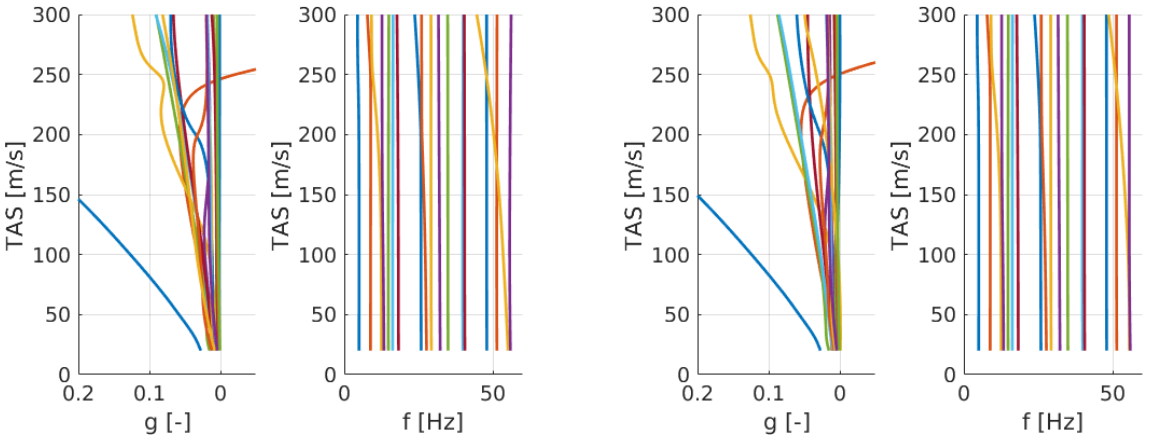

Figure 8: Flutter results with the small-disturbance CFD (left) and the corrected DLM (right) aerodynamics

Since the flutter results of the small-disturbance CFD and the Doublet-Lattice Method are very similar in this case, Figure 8 shows some minor corrections of the Doublet-Lattice results without any negative effect on the accuracy.

4.1.4 Other possible applications

Even in this subsonic case, the AIC-correction should be profitable for gust analyses, because it increases the accuracy of the force distribution along the components.

For other cases, especially in higher subsonic and at the beginning of the transonic regime, the need for a correction of the Doublet-Lattice aerodynamics increases and can then be covered by the current method.

4.2 Component-wise modal basis

4.2.1 Modal results

The objective set for this paper was to obtain a modal basis representing correctly the first 18 (3 rigid-body modes, 15 elastic modes) original antisymmetric eigenmodes of the OptiMALE configuration. Thus, the created component-wise modal basis had to be accurate for eigenfrequencies up to 50Hz. Therefore, all modes of the model with rigid T-tail on one side, and of the clamped elastic T-tail on the other side, were computed up to 60Hz. This led to 22 modes in the new built modal basis.

In order to validate the component-wise modal basis Φ, the mass- and stiffness-matrices of the OptiMALE configuration were generalized in terms of it. Then, an eigenvalue computation of these generalized structural matrices gave the rebuilt (normal) modeshapes and eigenvalues of the OptiMALE configuration in the following way. The square root of the eigenvalues are the circular frequencies associated to each eigenmode, whereas the obtained eigenvector matrix V can be used to create the rebuilt modal matrix Φ_{rebuilt} according to equation 5:

$$\Phi_{rebuilt} = \Phi \mathrm{V} \tag{5}$$

In order to compare the rebuilt modal basis with the original one, two criteria were used. First, the rebuilt and original modeshapes had to be matched to each other. In the present paper, a Modal Assurance Criterion (MAC) technique was used. Let $\overrightarrow{\varphi_i}$ and $\overrightarrow{\varphi_j}$ be two modeshapes (eigenvectors) to be compared, and M the mass matrix of the mass configuration. The following MAC will tend to 1 if these modeshapes are very similar and to 0 if they are not correlated.

$$MAC\left(\overrightarrow{\varphi_i}, \overrightarrow{\varphi_j}\right) = \frac{\left(\overrightarrow{\varphi_i}^T M \overrightarrow{\varphi_j}\right)^2}{\left(\overrightarrow{\varphi_i}^T M \overrightarrow{\varphi_i}\right)\left(\overrightarrow{\varphi_j}^T M \overrightarrow{\varphi_j}\right)} \tag{6}$$

Since this MAC-definition uses the mass matrix of the FEM-model, it is very efficient when comparing normal modes as presented in this paper. The fitting of the original and rebuilt bases can be seen in Figure 9.

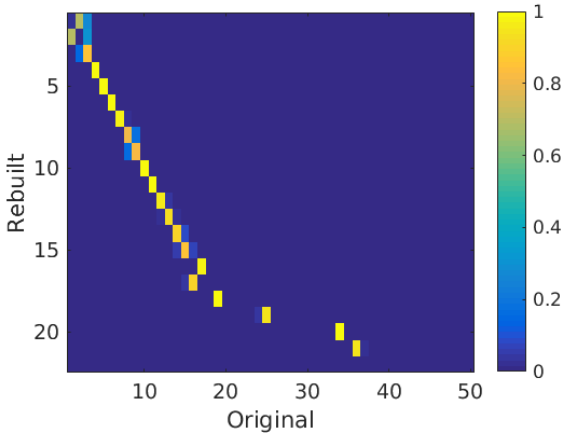

Figure 9: MAC results between rebuilt modes and original modes

Figure 9 shows a good match between original and rebuilt modeshapes. For the first three modes, the MAC criterion is not applicable since those eigenmodes are all associated to the same multiple eigenvalue (0). Both rigid-body modal bases show a high quality. Mode 8 and 9 seem to have some limited discrepancies. Mode 16 and 17 cross in frequencies, however, since these are very close to each other, this result is also acceptable. One can observe anyway that also more than the first 18 eigenmodes of the original modal basis can be captured. The original modes with no match are actually internal local modes (without any aerodynamic influence, therefore excluded from the component basis).

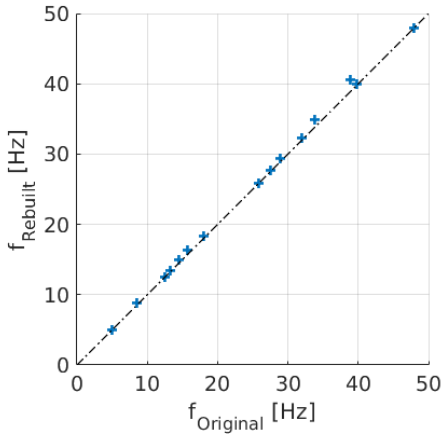

Figure 10: Frequency matching results between rebuilt modes and original modes

In a second step, the eigenfrequencies associated to these matched original and rebuilt modes are compared. This is presented graphically in Figure 10. The frequencies of the associated original and rebuilt modes match with high accuracy.

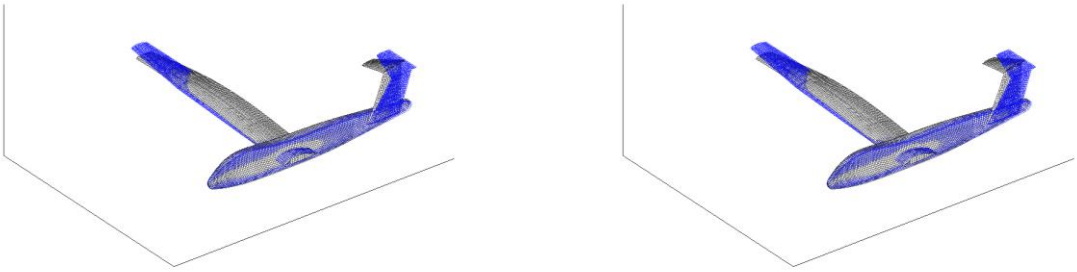

Figure 11: Second wing-bending mode (left: original modal basis, right: rebuilt)

In order to get a better impression of the quality of the results, the second wing-bending (Figure 11) and the first wing-torsional (Figure 12) modes are analyzed in more detail here. These modes have the highest participation in the flutter point presented in section 4.2.2.

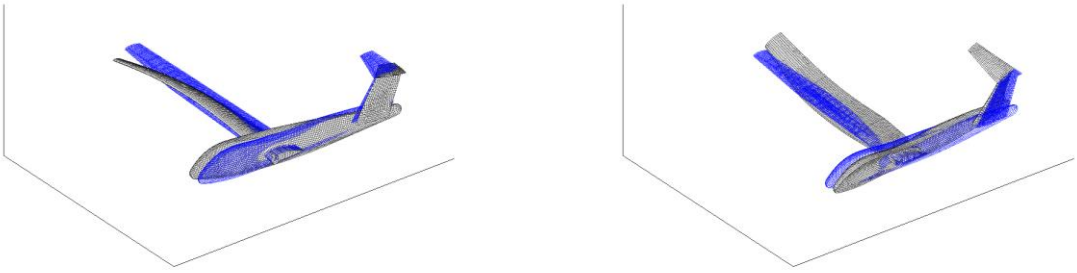

Figure 12: First wing-torsional mode (left: original modal basis, right: rebuilt)

Both modes have a MAC-value higher than 0.99 between the original and the rebuilt bases. This very high value of the MAC is confirmed by the graphical comparison of the modeshapes, while only the sign of the eigenvector can vary (as for the first torsional mode). The frequency difference lies around 3% for the second wing-bending and around 0.25% for the first torsion.

4.2.2 Flutter results

In order to validate the promising modal results, a flutter analysis with the non-corrected DLM-model was realized at Mach 0.4 and at Sea Level. In two analyses, the original antisymmetric modal basis with 18 modes and the component-wise modal basis with 22 modes were used (Figure 13).

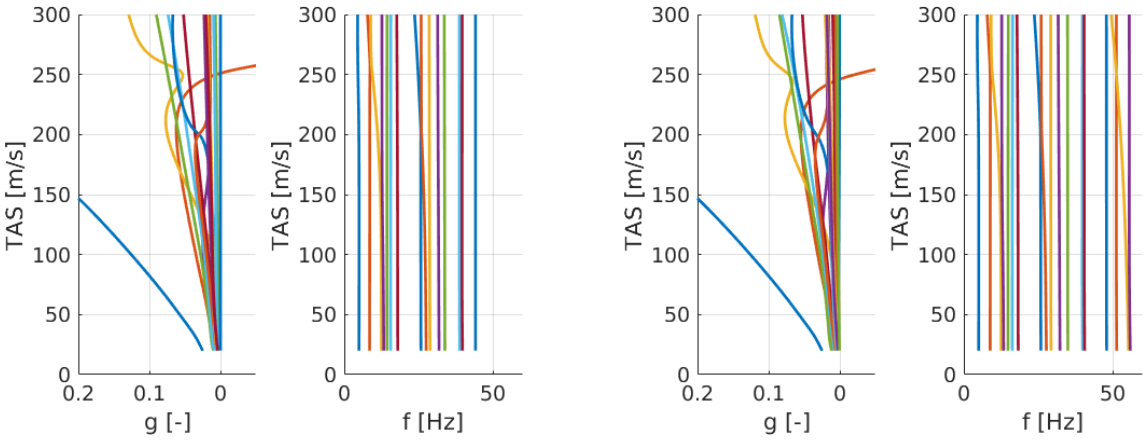

Figure 13: Flutter results (DLM) with the original (left) and the component-wise (right) modal bases

The flutter curves (Vg- and Vf-plots) of both modal bases show very similar characteristics, the same flutter mechanism and very limited differences in terms of the flutter speed (around 2%) and frequency (lower than 1%).

The presented results prove the component-wise basis to be a very accurate methodology that doesn't require a considerable increase in the number of modeshapes needed for obtaining similar results.

4.2.3 Other possible applications

The present methodology can also be combined with the AIC-correction technique in a very efficient way, if some component (such as the T-tail here) needs full small-disturbance CFD results whereas the rest of the aircraft can be simply modelled using DLM with AIC-correction. One should simply replace the related columns of the generalized aerodynamic forces (GAF) matrices with the computed small-disturbance CFD GAFs induced by these component modes. This hybrid method is not possible for the original modal basis where all components can be part of every eigenmode.

Another application is the resizing of some component (without changing its aerodynamic characteristics) that will in this case only require the recomputation of the new modal basis of this component and of the related small-disturbance CFD dataset. As an example, resizing the component T-tail would require the replacement of only 4 component modes, whereas the original basis (18 modes) would have to be recomputed completely. Since the number of small-disturbance CFD analyses is directly proportional to the number of considered eigenmodes, the expected gain of such a methodology is high.

4.3 Reuse of modal bases

In order to validate this approach, three fuel states were used for generating modal bases. For the first configuration, all fuel tanks are empty. The second one has all tanks half full, and the last one is the full fuel configuration.

The difference in overall mass between the empty and the full configuration lies around 40% of the full fuel mass, so that the effects on the modal and flutter results should be of some importance.

Each of the three modal bases was computed with 18 eigenmodes (3 rigid-body, 15 elastic modes).

4.3.1 Modal results

The MAC-criterion presented in section 4.2.1 is reused here, as well as the methodology for computing the eigenmodes of a modal basis using the generalized matrices of another one.

In this section the full-fuel modal basis is used to estimate the modal characteristics of the empty and of the half-full fuel configurations. The MAC-results are shown in Figure 14, whereas the matching of eigenfrequencies is presented in Figure 15.

Figure 14 shows a very good match of the elastic modes, especially for the half-full fuel configuration. The non-matched 18^{th} mode of the rebuilt empty configuration is actually not of importance, since the full-fuel mode associated to it was a local mode due to a lack of stiffness at the attachment of a fuel tank of the wing. The rigid-body modes Exhibit a very good agreement, and the MAC results for them are as in section 4.2.1 not applicable. This shows anyway that no user should expect computed rigid-body modes to have some specific orientation, unless some kind of supporting technique is applied. This orientation has no effect on the dynamic or aeroelastic stability or response computations, so no further work has been done on this subject in this paper.

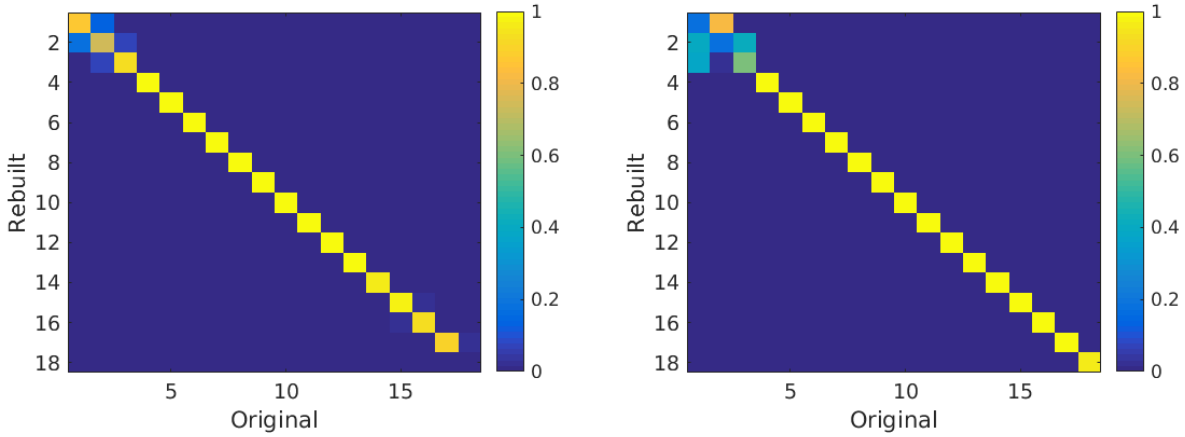

Figure 14: MAC results between rebuilt modes and original modes (left: empty fuel, right: half fuel)

The frequency comparison presented in Figure 15 shows also a good match for both cases. The rebuilt empty-fuel eigenfrequency has a maximum relative error of about 5% (for the last matched eigenmode), whereas this error lies under 2% for the half-fuel eigenfrequencies (also for the last eigenmode).

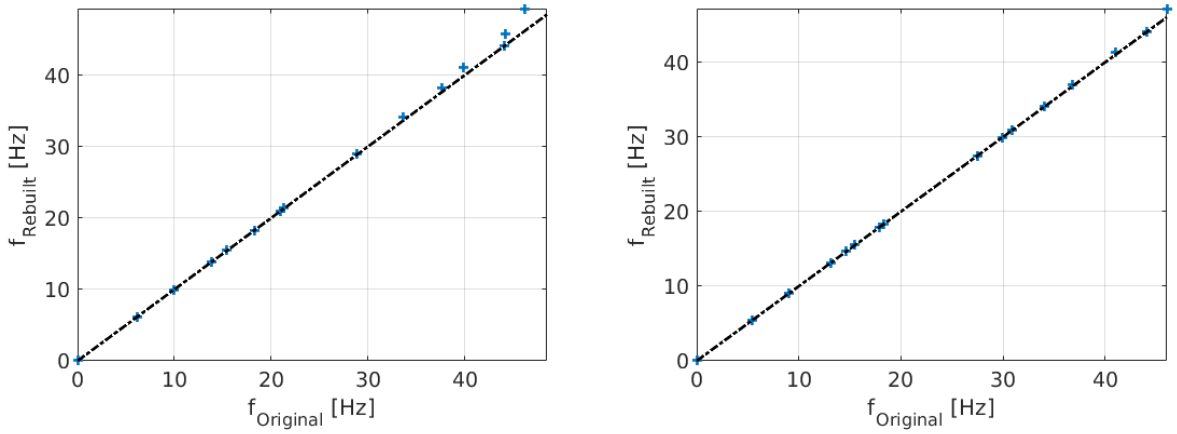

Figure 15: Frequency matching results between rebuilt modes and original modes (left: empty fuel, right: half fuel)

The results observed using the half-full and empty-fuel modal bases as references are even more accurate.

4.3.2 Flutter results

The flutter results (using Doublet-Lattice aerodynamics) are presented briefly in terms of flutter speed and frequency trend of the first antisymmetric flutter mode at Mach 0.4 at Sea Level (Figure 16). In all cases, this flutter mode is a coupling between the second bending mode and the first torsion mode of the wing.

The results in Figure 16 can be read as follows: each line represents the results of one out of the three mass states, whereas the abscissae denotes the modal basis in which the flutter results were computed. The cross represents the case where the used modal basis and the computed mass case match, and is therefore the reference configuration for each mass state.

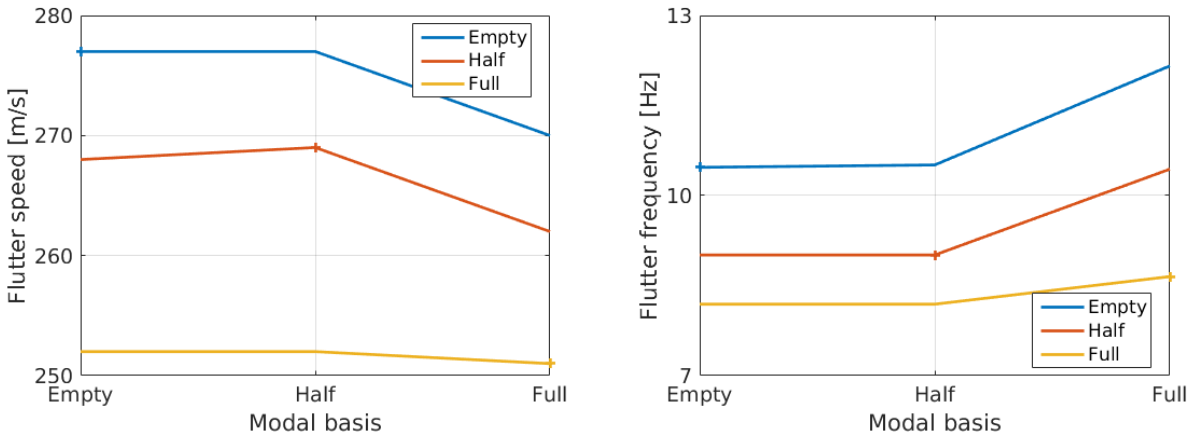

Figure 16: Flutter speed and frequency for the three fuel mass states of OptiMALE.

One can observe that using another modal basis has a limited effect on the flutter speed. Comparing the flutter frequencies, the authors conclude that it would be better to use the half-fuel or the empty-fuel modal basis in order to generalize the other mass states because the results obtained with the full-fuel modal basis for the empty- and half-fuel states were slightly less accurate. Then, only one modal dataset should be computed with small-disturbance CFD, leading to important savings in computational time at almost equivalent quality.

The results obtained with these three important mass variations demonstrate clearly that one or a few specific reference modal bases can be used in order to generalize the other mass states. Therefore the computational effort yielding an accurate small-disturbance CFD dataset can be reduced strongly without any important loss of accuracy.

4.3.3 Other applications

This methodology can also be used for gust analyses or aeroservoelastic problems, where the full flight-envelope has to be analyzed for several Mach numbers and (if necessary) for different flight-conditions (angle of attack, control surfaces or flaps positions). Reducing the number of modal bases used for the generation of full small-disturbance datasets is then also in later phases a very good and efficient practice.

5 CONCLUSIONS

All methodologies presented here proved their reliability, their accuracy and their saving potential for a more efficient use of small-disturbance CFD. They all rely on good engineering judgement and good practice and can considerably increase the flexibility of this still computationally intensive aerodynamic method.

6 ACKNOWLEDGEMENTS

The authors would like to thank Dr. Daniele Parisse from Airbus Defence and Space for his help at setting the mathematical basis of the AIC-correction presented here.

7 REFERENCES

[1] C. Vidy, L. Katzenmeier, M. Winter, C. Breitsamter, ”Verification of the use of small-disturbance CFD aerodynamics in flutter and gust analyses for simple to highly complex

configurations", International Forum on Aeroelasticity and Structural Dynamics, 2015, IFASD-2015-066.

[2] J.P. Giesing, T.P. Kalman, W.P. Rodden, "Correction Factor Techniques For Improving Aerodynamic Prediction Methods", NASA, 1976. NASA CR-144967.

[3] G.M.L. Gladwell, "Branch-Mode Analysis of Vibrating Systems", J. Sound Vib. (1964) I, 41-59

[4] E. Albano and P. Rodden, "A Doublet Lattice method for calculating lift distributions on oscillating surfaces in subsonic flows", *AIAA Paper*, No. 68-73, 1968.

[5] W. Rodden and E. Johnson, "MSC/NASTRAN Aeroelastic Analysis User's Guide", MSC, 1994.

[6] C. Weishäupl and B. Laschka, "Small Disturbance Euler Simulations for Delta Wing Unsteady Flows due to Harmonic Oscillations", *Journal of Aircraft*, Vol. 41, No. 4, 2004, pp. 782-789.

[7] A. Pechloff and B. Laschka, "Small Disturbance Navier-Stokes Method: Efficient Tool for Predicting Unsteady Air Loads", *Journal of Aircraft*, Vol. 43, No. 1, 2006, pp. 17-29.

[8] A. Pechloff and B. Laschka, "Small Disturbance Navier-Stokes Computations for Low Aspect Ratio Wing Pitching Oscillations", 26th Congress of the International Council of the Aeronautical Sciences, ICAS Paper 2008-2.10.3, Anchorage, AK, Sep. 2008.

[9] M. Iatrou, A. Allen, A. Pechloff, C. Breitsamter and B. Laschka, "Small Disturbance Euler-/Navier-Stokes Computations for Delta Wing Flap Oscillation", Meeting Proc. Flow Induced Unsteady Loads and the Impact on Military Applications, RTO-MP-AVT-123, Paper 16, Budapest, Hungary, April 25 – 28, 2005, pp. 16-1 – 16-20.

[10] K. C. Hall and E. F. Crawley, "Calculation of Unsteady Flows in Turbomachinery Using the Linearized Euler Equations", *AIAA Journal*, Vol. 27, No. 6, 1989, pp. 777-787.

[11] E. Kreiselmaier and B. Laschka, "Small Disturbance Euler Equations: Efficient and Accurate Tool for Unsteady Load Prediction", *Journal of Aircraft*, Vol. 37, No. 5, 2000, pp. 770-778.

[12] D. Fleischer, C. Vidy, M. Iatrou, C. Breitsamter, C. Weishäupl, "Linear Flutter Prediction For Low Aspect Ratio Wings Using A Small Disturbance Euler Method", International Forum on Aeroelasticity and Structural Dynamics, 2009, IFASD-2009-055.

[13] Y. Revalor, L. Daumas, N. Forestier, " Industrial use of CFD for loads and aero- servo-elastic stability computations at Dassault Aviation", 2011, IFASD-2011-061.

[14] J. R. Wright, J. Cooper, "Introduction to Aircraft Aeroelasticity and Loads", Aerospace Series, John Wiley & Sons, 2008

[15] C. Vidy, M. Iatrou, C. Weishäupl, D. Fleischer, M. Förster, C. Breitsamter, "Development of Aerodynamic Influence Coefficients based on CFD Codes for Aeroelastic Applications", International Forum on Aeroelasticity and Structural Dynamics, 2011, IFASD-2011-065.

[16] C. Vidy, M. Förster, M. Iatrou, C. Breitsamter, "Dynamic Stability and Response Analysis using a small-disturbance CFD Method", International Forum on Aeroelasticity and Structural Dynamics, 2013, IFASD-2013-25B.

[17] E. Kreiselmaier, „Berechnung instationärer Tragflügelumströmungen auf der Basis der zeitlinearisierten Eulergleichungen", Ph.D Dissertation,Inst. for Fluid Mechanics, Technische Universität München, Garching, Germany, July 1998.

[18] L. Katzenmeier, „Aeroelastische Untersuchungen an einer generischen MALE-Konfiguration unter Verwendung eines linearisiserten CFD-Euler-Verfahrens“, Bachelor Thesis, Lehrstuhl für Aerodynamik und Strömungsmechanik, Technische Universität München, Airbus Defence & Space, 2014.

[19] D. Fleischer, C. Breitsamter, “Efficient Computation of Unsteady Aerodynamic Loads Using Computational-Fluid-Dynamics Linearized Methods”, Journal of Aircraft, Vol. 50, No. 2, March-April 2013

COPYRIGHT STATEMENT